The UVES large program for testing fundamental physics II: constraints $\Delta\mu/\mu$ towards quasar HE 0027 − 1836

H. Rahmani[1], M. Wendt[2,3], R. Srianand[1], P. Noterdaeme[4], P. Petitjean[4],

P. Molaro[5,6], J. B. Whitmore[7], M. T. Murphy[7], M. Centurion[5], H. Fathivavsari[8],

S. D'Odorico[9], T. M. Evans[7], S. A. Levshakov[10,11], S. Lopez[12],

C. J. A. P. Martins[6], D. Reimers[2], and G. Vladilo[5]

[1] Inter-Univ. Centre for Astron. and Astroph., P.B. 4, Ganeshkhind, 411 007 Pune, India
[2] Hamburger Sternwarte, Uni. Hamburg, Gojenbergsweg 112, 21029 Hamburg, Germany
[3] Institut für Physik und Astronomie, Universität Potsdam, 14476 Golm, Germany
[4] IAP UMR 7095 CNRS, Uni. P. et M. Curie, 98 bis bvd Arago, Paris 75014, France
[5] INAF-Osservatorio Astronomico di Trieste, Via G. B. Tiepolo 11, 34131 Trieste, Italy
[6] Centro de Astrofísica, Universidade do Porto, Rua das Estrelas, 4150-762 Porto, Portugal
[7] C.A.S Swinburne University of Technology, Hawthorn, VIC 3122, Australia
[8] Dep. of Theoretical Physics and Astrophysics, Univ. of Tabriz P.O. Box 51664, Iran
[9] ESO, Karl Schwarzschild-Str. 1 85748 Garching, Germany
[10] Ioffe Phy.-Tec. Inst., Polytekhnicheskaya, Str. 26, 194021 St. Petersburg, Russia
[11] St. Petersburg Electrot. Uni. 'LETI', Prof. Popov Str. 5, 197376 St. Petersburg, Russia
[12] Departamento de Astronomia, Universidad de Chile, Casilla 36-D, Santiago, Chile

Abstract. We study the variation of proton-to-electron mass ratio, μ, using the H_2 absorption lines from the $z_{abs} \sim 2.4018$ DLA system towards HE 0027 − 1836 observed with the VLT/UVES as a part of the ESO Large Program for testing fundamental physics. A cross-correlation analysis between individual exposures and the combined spectrum and asteroid observations show the existence of a possible wavelength dependent drift in the UVES observation. We find that a two component Voigt profile model can best fit the H_2 absorption profile and give $\Delta\mu/\mu = -2.5 \pm 8.1_{stat} \pm 6.2_{sys}$ ppm. When we apply the correction to the wavelength dependent velocity drift we find $\Delta\mu/\mu = -7.6 \pm 8.1_{stat} \pm 6.3_{sys}$ ppm.

Key words. galaxies: quasar: absorption line – quasar: individual: HE 0027 − 1836

1. Introduction

Most of the fundamental physical theories rely on fundamental constants that their values are assumed to be constant independent of space and time. The fine structure constant, α, and the proton-to-electron mass ratio, μ, are two of such constants that are frequently measured experimentally. While laboratory experiments exclude any significant variation of fundamental constants, it is neither observationally nor experimentally excluded that the fundamen-

tal constants can vary over cosmological times and scales. Therefore, constraining the variation of fundamental constant have important impact on fundamental physics (See Amendola et al. 2012).

It is known that the energy of rovibronic transitions in a molecule like H_2 is sensitive to the value of μ. The frequency of the rovibronic transitions in Born-Oppenheimer approximation can be written as,

$$\nu = c_{\text{elec}} + c_{\text{vib}}/\sqrt{\mu} + c_{\text{rot}}/\mu \qquad (1)$$

where c_{elec}, c_{vib}, and c_{rot} are some numerical coefficients related, respectively, to electronic, vibrational and rotational transitions. Therefore, by comparing the wavelength of the molecular transitions detected in quasar spectra with their laboratory values one can measure the variation in μ (i.e. $\Delta\mu/\mu \equiv (\mu_z - \mu_0)/\mu_0$ where μ_z and μ_0 are the values of μ at redshift z and today) over cosmological time scales (Thompson 1975). Being the most abundant molecule, the Lyman and Werner absorption lines of H_2 seen in quasar absorption spectra have been frequently used to constrain the variation of μ. However, only $\sim 10\%$ of high redshift DLAs present H_2 (Noterdaeme et al. 2008) a few out of which are useful for probing the variation of μ.

Any variation of μ translates to shifts in the observed wavelengths of H_2 transitions. Such shift will be different for different H_2 lines and parametrized as

$$\lambda_i = \lambda_i^0 (1 + z_{\text{abs}})\left(1 + K_i \frac{\Delta\mu}{\mu}\right), \qquad (2)$$

where λ_i^0 is the rest frame wavelength of the transition, λ_i is the observed wavelength, K_i is the sensitivity coefficient of i'th transition, and z_{abs} is the redshift of the H_2 absorber. Eq. 2 can be presented as

$$z_{\text{red}} \equiv \frac{(z_i - z_{\text{abs}})}{(1 + z_{\text{abs}})} = K_i \frac{\Delta\mu}{\mu} \qquad (3)$$

that shows $\Delta\mu/\mu$ is the slope of the line fitted to z_{red} vs K_i. This is the method frequently used in the literature to constrain the variation of μ (e.g. Ubachs 2007; Wendt & Molaro 2012). All the $\Delta\mu/\mu$ measurements in the literature are
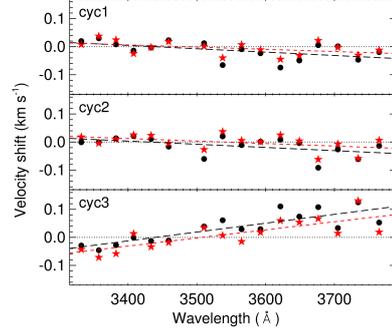
Fig. 1. Velocity offsets between the combined spectrum of all exposures and the combined spectrum for each observing cycle. The long-dashed lines show the line fitted to these shifts. The asterisks are the results after excluding EXP19 where the short-dashed lines show the line fitted to them.

consistent with a non-variation of μ at the level of $\Delta\mu/\mu < 10^{-5}$.

We report the analysis of the H_2 absorption in z=2.4018 DLA towards HE $0027 - 1836$ (Noterdaeme et al. 2007) with extreme care using the Ultraviolet and Visual Echelle Spectrograph mounted on the Very Large Telescope (VLT/UVES) spectra taken as part of the UVES large programme (LP) for testing the fundamental physics (Molaro et al. 2013). Here we present a summary of this analysis while the full detail can be found in Rahmani et al. (2013).

2. Observations and data reduction

Spectroscopic observations of HE $0027 - 1836$ were carried out using VLT/UVES (Dekker et al. 2000) Unit Telescope (UT2) 8.2-m telescope at Paranal (Chile) (as part of programme 185.A-0745 "*The UVES Large Program for testing Fundamental Physics*" Molaro et al. 2013). All the exposures are taken in 390+580 setting and followed by attached mode ThAr calibration lamps. A slit width of $0.8''$ and CCD readout with no binning were used for all the observations, resulting in a pixel size of $\approx$ 1.3 - 1.5 km s^{-1} on the BLUE CCD and spectral resolution of $\approx$ 60,000. The observation is comprised of 19 exposures totaling 33.3 hours

of exposure time distributed in three observing cycles from 2010 – 2012.

We have used UVES Common Pipeline Library (CPL) data reduction pipeline release 5.3.1 to reduce the raw spectra. Dispersion solutions for the wavelengths are found using 4th order polynomials by using more than 700 ThAr lines. The rms error found to be in the range of 40 – 50 m s^{-1} with zero average. To avoid rebinning we use the final un-rebinned CPL product for each order. We apply the wavelength solutions to each order and merge them in the overlapping regions using a weighted mean. Our final combined spectrum of all exposures has a SNR of $\sim$ 30 at $\sim$ 2800 Å.

Fig. 2. The velocity shift measurements using cross-correlation analysis between solar and asteroids spectra. The solid line in each panel shows the fitted line to the velocities. The $\Delta\mu/\mu$ corresponding to the slope of the fitted straight line is also given in each panel.

3. Systematic errors in the UVES wavelength scale

Having 19 exposures distributed over 3 years allows a detail study of possible systematic uncertainties in the wavelength calibration. We make use of a cross-correlation analysis to probe any of such systematics. In a cross-correlation analysis between individual exposures and the final combined spectrum we find that apart from EXP19 (with a velocity offset of $\lesssim$ 200 m s^{-1}) all exposures show constant offsets consistent with zero (See Fig. 2 of Rahmani et al. 2013). A similar cross-correlation analysis after excluding EXP19 from the combined spectrum shows this exposure can have a constant offset shift of 800 m s^{-1} that varies over different orders. As a result we exclude this exposure in the rest of our analysis.

To further probe the possible systematic errors we make combined spectra of the data in each cycle and cross-correlate them with the combined spectrum. As presented in Fig. 1 this analysis reveals the presence of a wavelength dependent velocity offset in the data taken in 2012. To confirm such a finding we make use of the spectra of asteroids observed with UVES.

3.1. Analysis of asteroids spectra observed with UVES

Asteroids are respectively bright objects ($m <$ 10 mag) with their spectra being filled of solar absorption lines over our interested range of wavelength. This makes these objects to be suitable probes for testing the accuracy of wavelength calibration (Molaro et al. 2008). We search in UVES archival data for asteroids observed in 390 UVES setting that are also close in time to our quasar observations. We find UVES observations of IRIS, CERES, and EROS distributed in 2010, 2011, and 2012. We further include the IRIS 2006 observations that are analyzed by Molaro et al. (2008).

We follow the already mentioned procedure for reducing the asteroids exposures. However, we do not make combined spectrum for any of the asteroids as we have enough SNR in individual exposures. A cross-correlation analysis between spectra of asteroids separated up to few months do show a stable wavelength scale of the UVES. We further confirm such stability in the range of 2010 – 2011 by comparing CERES spectra taken in October 2010 and October 2011. However, we find a clear wavelength dependent trend when comparing 2012 observations of IRIS with its 2006 observations. This trend is similar to what
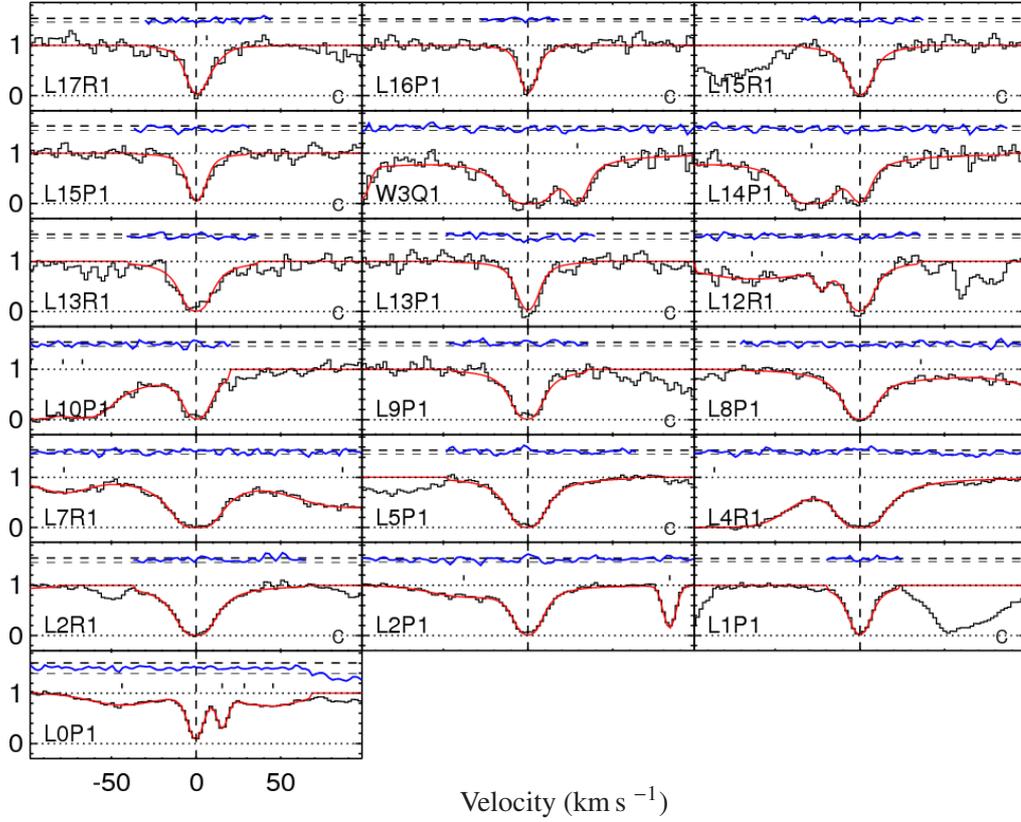
Fig. 3. Absorption profile of H_2 transitions of $J = 5$ level and the best fitted Voigt profile. The normalized residual (i.e. ([data]−[model])/[error]) for each fit is also shown in the top of each panel along with the 1-σ line. We present the clean absorption lines by putting a letter "C" in the right bottom of these transitions.

we have already seen in 2012 spectrum of HE 0027 − 1836. While confirming the existence of a wavelength dependent drift in 2012 observations of the UVES we can not yet quantify its amplitude absolutely. We require an independent highly accurate reference spectra not taken with UVES as a reference. We make use of solar spectra from Kurucz (2006) as such a reference and cross-correlate the asteroids individual spectra with the solar spectrum. The results of such an analysis is presented in Fig. 2. Different symbols in each panel correspond to asteroids exposures obtained within couple of days. A mean velocity offset is subtracted from each panel to bring the velocity

level to zero. Qualitatively, one sees a positive slope in all cases. Clearly EROS and IRIS spectra taken in 2012 show the largest slopes.

As wavelength dependent velocity shifts can mimic a non-zero $\Delta\mu/\mu$ it is important to translate the observed trend to an apparent $\Delta\mu/\mu$ in each case. To do so we carry out the following exercise: (1) Fitting a line to the velocity offset as $\Delta v(\lambda)$ to get the offset Δv and $\sigma_{\Delta v}$ at the observed wavelengths of our interested H_2 lines, (2) generating 2000 Gaussian realizations of each $\Delta v(\lambda)$ with $\sigma = \sigma_{\Delta v}$, (3) a $\Delta\mu/\mu$ measurement for each of 2000 realizations, and (4) finding the mean and 1-σ of the distribution as the systematic $\Delta\mu/\mu$ and its er-
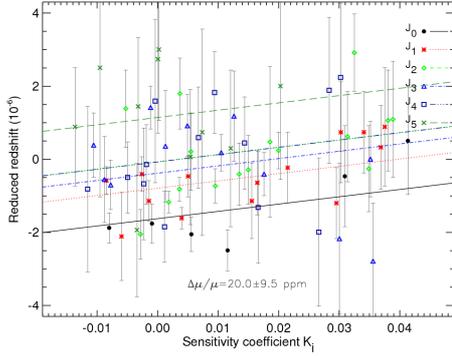
Fig. 4. Reduced redshift vs the K_i for all the fitted H_2 lines in the case of combined spectrum of all exposures except EXP19. Lines from different J-levels are plotted with different symbols. The best fitted linear line for different J-levels with the constraint that the slope should be same is also shown.

Table 1. Results of the Voigt profile analysis for different J-levels in HE 0027 − 1836.

J-level	N	z	σ_z km s^{-1}	δv km s^{-1}
(1)	(2)	(3)	(4)	(5)
0	6	2.4018452	0.07	0.00
1	14	2.4018486	0.05	0.30
2	16	2.4018499	0.07	0.41
3	12	2.4018522	0.08	0.62
4	13	2.4018513	0.11	0.54
5	10	2.4018550	0.15	0.87

Column (1): indices for different rotational levels. Column (2): number of transitions in the given J-level Column (3): mean weighted redshift of all transitions having same J-level. Column (4): redshift error in km s^{-1}. Column (5): redshift difference between the given J-level and $J = 0$ in km s^{-1}.

ror. In Fig. 2 we present the systematic $\Delta\mu/\mu$ for each of the asteroids observation. The systematic $\Delta\mu/\mu$ can vary from (2.5 ± 2.5) ppm for CERES 2010 to $\gtrsim 13$ ppm for EROS and IRIS 2012. This is a clear confirmation of our finding that UVES data acquired in 2012 has large wavelength drift. As the amplitude of the systematic $\Delta\mu/\mu$ can be larger than the statistical errors of $\Delta\mu/\mu$ measurements using H_2 lines it is important to remove these systematics from the data.

In summary our cross-correlation analysis shows the existence of a large velocity offset in EXP19 with respect to the rest of the data. Therefore, we exclude this exposure from our combined spectrum. Furthermore, our analysis reveals the presence of wavelength dependent velocity shifts that is significantly larger in 2012 observation.

4. Constraining $\Delta\mu/\mu$

The $z = 2.4018$ DLA towards HE 0027 − 1836 produces more than 100 H_2 absorption lines in the observed wavelength range of 3330 Å to 3800 Å spanning different rotational states from $J = 0$ to $J = 6$. The absorption lines from $J = 6$ are too weak to lead to any reasonable redshift estimation. Therefore, we do not use this rotational level for $\Delta\mu/\mu$ measurements.

However, for the rest of rotational levels we detect several absorption lines with wide ranges of oscillator strengths. This allows for a very reliable estimation of fitting parameters and associated errors though the absorption profiles are very narrow. We have confirmed the robustness of the VPFIT estimated errors in our fitting by a Monte Carlo simulation over 100 realization (e.g. Fig. 8 in Rahmani et al. 2013). By inspecting the spectrum we choose 71 H_2 lines that are suitable for measuring $\Delta\mu/\mu$ out of which 24 are mildly contaminated by Lyα forest lines or metal lines of the DLA. We include these contaminated lines in our analysis while simultaneously modeling the contamination through multi-component Voigt profiles. Fig. 3 shows the best single component fit to the absorption profiles of $J = 5$ lines.

$\Delta\mu/\mu$ can be measured via two approaches using H_2 absorption lines: (i) linear regression analysis of $z_{\rm red}$ vs K_i with $\Delta\mu/\mu$ as the slope or (ii) using $\Delta\mu/\mu$ as an additional parameter in the VPFIT. We employ both the methods to derive $\Delta\mu/\mu$ from our data considering two cases: (i) single component Voigt profile fit and (ii) two component fit. While doing regression analysis we use a bootstrap technique to estimate the uncertainty in $\Delta\mu/\mu$. This is done as the systematic errors found in the data make

the distribution of the redshifts to be larger than the redshift errors.

4.1. $\Delta\mu/\mu$ measurements using z-vs-K analysis

We fit the H$_2$ lines using a single component Voigt profile allowing b-parameters to be different for different J-levels.

The estimated redshifts for different J-levels for such a fit is presented in Table 1. As shown in this table the mean redshift of different J-levels are different. Therefore, while carrying out the regression analysis we fit lines of different intercepts but with the same slope. The best fitted value for $\Delta\mu/\mu$ is 20.0 ± 9.3 ppm (See column 2 of the last row in Table 2).

As the wavelength dependent velocity shift is found to be minimum in the case of first two cycles we measured the $\Delta\mu/\mu$ using only the data obtained in the first two cycles (i.e. 13 exposures and total integration time of $\sim$ 23 hrs). We call this sub-sample as "1+2". The results of the $\Delta\mu/\mu$ measurement for this case is $+10.7\pm11.4$ ppm. As expected the mean $\Delta\mu/\mu$ obtained from this sub-sample is less than the one obtained for the whole sample. The amount of observing time in different cycles are respectively 10.4 hours, 12.5 hours, and 10.4 hours for the first, second, and third cycle. Therefore, we also measured $\Delta\mu/\mu$ using data obtained in individual cycles. We get $\Delta\mu/\mu = -1.7 \pm 16.3$ ppm, $+30.2 \pm 12.2$ ppm and $+41.6 \pm 19.5$ ppm respectively for the first, second and third cycles. The progressive increase in the mean $\Delta\mu/\mu$ is consistent with what we notice in Fig. 2 for the asteroids.

Here we correct the wavelength scales of the individual exposures based on the results of the closest asteroid observation. We further make a new combined spectrum and carry out a $\Delta\mu/\mu$ measurements. Results of $\Delta\mu/\mu$ measurements after applying the drift correction for different cases are summarized in column 3 of Table 2. We find $\Delta\mu/\mu = +15.0\pm9.3$ ppm for the combined data after applying corrections. Clearly an offset at the level of 5 ppm comes from this effect alone in the combined data.

We notice that because of severe blending, z-vs-K method cannot be easily applied to the

two component fit. In the following section we obtain $\Delta\mu/\mu$ directly from VPFIT for both single and two component fits.

4.2. $\Delta\mu/\mu$ measurements using VPFIT

Columns 4 – 13 in Table 2 summarize the $\Delta\mu/\mu$ results for the case where $\Delta\mu/\mu$ is a fitting parameter in VPFIT. When we consider the single component fit we find $\Delta\mu/\mu = +21.8\pm6.9$ ppm for the full sample with a reduced χ^2 of 1.188 (see columns 4 and 5 in Table 2) which is consistent with the results from z-vs-K analysis. We further find $\Delta\mu/\mu = +18.8\pm7.7$ ppm for the combined spectrum of the first two cycles. This also confirms our finding that the addition of third year data increases the measured mean of $\Delta\mu/\mu$. When we use the corrected spectrum for the full sample we get $\Delta\mu/\mu = +15.6\pm6.9$ ppm. The $\Delta\mu/\mu$ measurements for different cases after applying the correction and the corresponding reduced χ^2 are given in columns 7 and 8 respectively. The statistical errors from the VPFIT are smaller than those obtained from the bootstrap technique in the z-vs-K analysis. We need to further associate 6.2 ppm extra error to the VPFIT error to recover the z-vs-K error. Therefore, we will quadratically add 6.3 ppm of systematic error to the final statistical error of the best model obtained using VPFIT. Column 6 in Table 2 gives the Akaike information criteria (AIC; Akaike 1974) corrected for the finite sample size as given in the Eq. 4 of King et al. (2011). We can use AICC in addition to the reduced χ^2 to discriminate between the models.

Columns 9 – 13 of Table 2 summarizes the results of the two component Voigt profile fits where $\Delta\mu/\mu$ is a free parameter of the fits. We find $\Delta\mu/\mu = -2.5 \pm 8.1$ ppm with a reduced χ^2 of 1.177 and $\Delta\mu/\mu = -7.6 \pm 8.1$ ppm with a reduced χ^2 of 1.171 respectively for uncorrected and corrected spectrum. The χ^2_{red} is lower for the case of two component fit and AICC is 52 in favour of two component fit when comparing them with the statistics of the single component fit. Therefore, we consider the $\Delta\mu/\mu$ from the two component fits as our final result. However, as already discussed we add a 6.3 ppm to its error as an estimate of systematic error.

Table 2. $\Delta\mu/\mu$ measurement for each cycle in 10^{-6} unit.

	z-vs-K			VPFIT								
	1-component			1-component					2-components			
(1)	(2)	(3)	(4)	(5)	(6)	(7)	(8)	(9)	(10)	(11)	(12)	(13)
cycle	original	corrected†	original	χ^2_ν	AICC	corrected†	χ^2_ν	original	χ^2_ν	AICC	corrected†	χ^2_ν
1	−1.7 ±16.3	−4.6 ±16.8	+21.1±10.0	1.037	6302	+19.8± 9.9	1.029	−11.7±12.2	1.032	6295	−12.1±11.8	1.022
2	+30.2±12.2	+26.7±12.7	+15.5±10.5	0.974	5948	+10.0±10.5	0.972	+10.7±11.9	0.969	5936	+5.2 ±11.9	0.967
3*	+41.6±19.5	+30.1±19.0	+30.2±14.3	0.932	5705	+14.5±12.5	0.927	+12.9±13.5	0.912	5614	−0.8 ±13.4	0.907
1+2	+10.7±11.4	+13.8±10.2	+18.8± 7.7	1.128	6825	+15.8± 7.7	1.123	+0.8 ± 8.6	1.120	6794	−1.5 ± 8.7	1.115
1+2+3*	+20.0± 9.3	+15.0±9.3	+21.8± 6.9	1.188	7167	+15.6± 6.9	1.179	−2.5 ± 8.1	1.178	7115	−7.6 ± 8.1	1.171

* result of the cases that EXP19 is excluded.

† results after correcting the systematics based on the solar-asteroid cross-correlation.
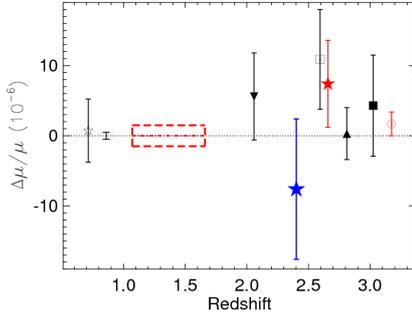
Fig. 5. A comparison between constraint obtained on $\Delta\mu/\mu$ in this work and those in the literature. Measurements at $2.0 < z < 3.1$ are based on the study of H_2 absorption systems. The filled larger blue star shows our result and the smaller red star shows the result from Albornoz Vásquez et al. (2013). The filled upward triangle and the empty and filled squares are respectively from King et al. (2011), King et al. (2008) and Wendt & Molaro (2012). The downwards filled triangle is $\Delta\mu/\mu$ measurement from and Malec et al. (2010). The solid box and the open circle present the results respectively by Rahmani et al. (2012) and Srianand et al. (2010) based on a comparison between 21-cm and metal lines in Mg II absorbers under the assumption that α and g_p have not varied. The $\Delta\mu/\mu$ at $z < 1$ are based on ammonia and methanol inversion transitions that their 5σ errors are shown. The measurement at $z \sim 0.89$ is from Bagdonaite et al. (2013). The $\Delta\mu/\mu$ at $z \sim 0.684$ is from Murphy et al. (2008).

5. Discussion

We have analyzed an H_2 absorption system at $z_{abs} = 2.4018$ along the line of sight of HE 0027 − 1836 to constrain the possible variation of μ. We have carried out a very detail analysis of asteroids observed with VLT/UVES to understand the systematic errors of the UVES wavelength calibration. Solar-asteroid cross-correlation provides a technique to somehow quantify the extent of the detected systematic error and its contribution to measured $\Delta\mu/\mu$. We measure $\Delta\mu/\mu = (−7.6 \pm 8.1_{stat} \pm 6.3_{sys})$ ppm after correcting our data for the measured systematics. Our constrain is consistent with no variation of μ at a level of one part in 10^5 over last 10.8 Gyr (see Fig. 5).

Fig. 5 summarizes the constraint on μ obtained based on different approaches. Measurements at $2.0 < z < 3.1$ obtained using H_2 absorption line analysis and most of them are positive, though consistent with zero. Interestingly, the analysis of asteroids also presents the existence of systematics in UVES that can increase the value of $\Delta\mu/\mu$ towards positive values. As the majority of these measurement are from VLT/UVES one should be careful while making an overall statistical conclusion out of them.

References

Akaike, A. 1974, IEEE Tran. Autom. Control, 19, 716

Albornoz Vásquez D., Rahmani H., Noterdaeme P. et al. 2013, submitted to A&A

Amendola, L., Leite, A. C. O., Martins, C. J. A. P., et al. 2012, Phys. Rev. D, 86, 063515

Bagdonaite, J., Jansen, P., Henkel, C., et al. 2013, Science, 339, 46

Balashev, S. A., Petitjean, P., Ivanchik, A. V., et al. 2011, MNRAS, 418, 357

Dekker, H., D'Odorico, S., Kaufer, A., Delabre, B., & Kotzlowski, H. 2000, Proc. SPIE, 4008, 534

D'Odorico, S., Cristiani, S., Dekker, H., et al. 2000, Proc. SPIE, 4005, 121

King, J. A., Webb, J. K., Murphy, M. T., et al. 2008, Phys. Rev. Lett., 101, 4

King, J. A., Murphy, M. T., Ubachs, W., et al. 2011, MNRAS, 417, 3010

Kurucz, R. L. 2006, `arXiv:0605029`

Malec, A. L., Buning, R., Murphy, M. T., et al. 2010, MNRAS, 403, 1541

Molaro, P., Levshakov, S. A., Monai, S., et al. 2008, A&A, 481, 559

Molaro, P., Centurión, M., Whitmore, J. B., et al. 2013, A&A, 555, 68

Murphy, M. T., Flambaum, V. V., Muller, S., & Henkel, C. 2008, Science, 320, 1611

Noterdaeme, P., Ledoux, C., Petitjean, P., et al. 2007, A&A, 474, 393

Noterdaeme, P., Ledoux, C., Petitjean, P., & Srianand, R. 2008a, A&A, 481, 327

Rahmani, H., Srianand, R., Gupta, N., et al. 2013, MNRAS, 425, 556

Rahmani, H., Wendt, M., Srianand, R., et al. 2013, `arXiv:1307.5864`

Srianand, R., Gupta, N., Petitjean, P., et al. 2010, MNRAS, 405, 1888

Thompson, R. I. 1975, Astrophys. Lett., 16, 3

Ubachs, W., Buning, R., Eikema, K. S. E., & Reinhold, E. 2007, J. Molec. Spec., 241, 155

Wendt M. & Molaro P. 2012, A&A, 541, 69